

# **Mitosis, Cytoskeleton Regulation, and Drug Resistance in Receptor Triple Negative Breast Cancer**

Alexandre Matov<sup>1,†</sup>

<sup>1</sup> DataSet Analysis LLC, 155 Jackson St, San Francisco, CA 94111

<sup>†</sup> Corresponding author:  
email: [matov@datasetanalysis.com](mailto:matov@datasetanalysis.com)

**Key words:** Receptor-Negative Breast Cancer, End-Binding Protein, Microtubule Dynamics, Mitotic Spindle, Motion Tracking, Drug Development

## ABSTRACT

Methods for personalizing medical treatment are the focal point of contemporary biomedical research. In cancer care, we can analyze the effects of therapies at the level of individual cells. Quantitative characterization of treatment efficacy and evaluation of why some individuals respond to specific regimens, whereas others do not, requires additional approaches to genetic sequencing at single time points. Methods for the continuous analysis of changes in phenotype, such as *in vivo* and *ex vivo* morphology and motion tracking of cellular proteins and organelles, over time-frames spanning the minute-hour scales, can provide important insights into patient treatment options.

Despite improvements in the diagnosis and therapy of many types of breast cancer (BC), many aggressive forms, such as receptor triple-negative cancers, are associated with the worst patient outcomes; though initially effective in reducing tumor burden for some patients, acquired resistance to cytotoxic chemotherapy is almost universal, and there is no rationale for identifying intrinsically drug-resistant and drug-sensitive patient populations before initiating therapy. During cell division, the receptor triple-negative MDA-MB-231 mitotic spindles are the largest in comparison to other BC cell lines. Many of the MDA-MB-231 spindles exhibit rapid lateral twisting during metaphase, which remains unaffected by knockdown of the oncogene Myc and treatment with inhibitors of the serine/threonine-protein kinase B-Raf and the epidermal growth factor receptor (EGFR), alone or in any combination.

The MDA-MB-231 cells are the most aggressive and rapidly form metastatic tumors in xenograft transplant models, and exhibited very high proliferation rates when plated as three-dimensional cultures in Matrigel. Quantitative image analysis of microtubules (MTs) in six BC cell lines - MDA-MB-231 (receptor negative), HCC-1143 (receptor negative), HCC-3153 (receptor negative), ZR75B (estrogen receptor-positive), LY2 (progesterone receptor-positive), HCC-1428 (estrogen receptor-positive, progesterone receptor-positive) - demonstrated that the rotational spindle rocking of MDA-MB-231 cells

during metaphase appears coupled with a significant increase in MT polymerization rates during interphase, which likely shortens interphase and accelerates cell cycle progression and mitotic entry. Unlike the uniform treadmilling rates of about 21  $\mu\text{m}/\text{min}$  in kinetochore MTs during metaphase we measured across cell lines, MDA-MB-231 cells in interphase exhibit the fastest MT polymerization dynamics of about 19  $\mu\text{m}/\text{min}$  and this is coupled with abnormal mitotic spindle oscillations of almost 30  $\mu\text{m}/\text{min}$ . This aberrant behavior in MDA-MB-231 spindles may represent a therapeutically targetable disrupted mechanism of spindle positioning in receptor triple-negative breast cancer (TNBC) cells leading to tumor aggressiveness. In this manuscript, we outline a strategy for the selection of the most optimal tubulin inhibitor based on the ability to affect MT dynamics.

## INTRODUCTION

When epithelial cells become neoplastic, that is reflected in changes in their ability to remodel their cytoskeleton and respond to drug treatment. The cellular highways, which stretch from the nucleus to the cell cortex, are the MTs. MTs are essential polymer filaments composed of tubulin subunits that organize and rearrange the interior of the cell (Inoue, 1959; Inoue and Salmon, 1995; Lyle et al., 2009a; Lyle et al., 2009b). They play indispensable roles in several cellular processes such as migration, mitosis, and internal transport, processes critically involved in cancer metastasis and proliferation. MTs are structurally stiff but dynamic. Their tendency to rapidly extend and retract in a stochastic way is termed dynamic instability of MT plus tips or plus ends (Mitchison and Kirschner, 1984). This dynamicity allows a cell to utilize MTs in diverse functional contexts, one of which is mitosis. Within the spindles, MTs undergo a process termed treadmilling (Maddox et al., 2003) during which the plus ends are located in proximity to the chromosomes at the metaphase plate, where MTs add dimers or polymerize, and the minus ends are located outward toward the two poles, from where the MTs remove dimers or depolymerize at similar rates. These MT-based structures align duplicated chromosomes near the cell center and ultimately segregate the copies into each of the daughter cells. In interphase, MTs are the freeways of the cellular

transport infrastructure. Failure to maintain the appropriate MT network in normal physiology is a hallmark of cancer (Hanahan and Weinberg, 2000; Hanahan and Weinberg, 2011) and a number of other diseases. Tubulin inhibitors bind to MTs and induce the MTs to modify their intercellular organization. Changing the arrangement of MTs alters how and where cellular signals are delivered which, in turn, changes MT and cellular homeostasis.

Our objective has been to elucidate the mechanisms of regulation by which cancer cells affect MT organization and how they affect susceptibility of the cell to tubulin inhibitors. To achieve this goal, we have developed software tools that allow us to look at MTs, as well as key cellular proteins, and measure how they change after drug treatment in living cells in real time (Matov, 2024b). Because tubulin inhibitors are already widely used for treatment of many solid tumors, elucidating the mechanisms behind MT organization in cancer cells of epithelial origin could identify putative targets. To best benefit individual patients, one will ultimately need a procedure to test the drugs *ex vivo* within a time frame suitable in the context of the patient treatment plan. In the Clevers lab (Hubrecht Institute, NL), the pioneers of the organoid technology, for a decade there has been an organoid-based test in cystic fibrosis that delivers results in about two weeks (Clevers and Bender, 2015). A major goal is to transfer this technology to oncology, which would allow to analyze MTs dynamically in patient-derived cancer cells during *ex vivo* treatment and, in doing so, the clinical use of MT dynamics as a biomarker for drug susceptibility.

## **MITOSIS IN BREAST CANCER CELLS**

Aggressive forms of BC, such as receptor triple-negative cancers and estrogen receptor-positive cancers of the luminal B molecular subtype, are associated with worse patient outcome (Maqbool et al., 2022). Though initially effective in reducing tumor burden for some BC patients, resistance to MT-targeting systemic therapy is universal and there is no rationale for identifying drug-sensitive and -resistant patient populations prior to initiating therapy. The signaling molecules that interact with MTs, as well as the

multiple effects on signaling pathways that destabilize or hyper-stabilize MTs, indicate that MTs are likely to be critical to the spatial organization of signal transduction. MTs are also affected by signaling pathways and this contributes to the transmission of signals to downstream targets (Gundersen and Cook, 1999). Many mechanistic models have been proposed to describe drug resistance to tubulin inhibitors (Orr et al., 2003), the most common of which are: (i) resistance due membrane-pump overexpression (Robert, 1999), (ii) resistance due tubulin-isotype composition (Haber et al., 1995; Kanakkanthara et al., 2011; Ranganathan et al., 1998), (iii) resistance due mutations in drug binding sites (Giannakakou et al., 2000; Giannakakou et al., 1997) as well as regulatory microRNA (Kanakkanthara and Miller, 2012). Evidence for these models stems largely from work with tissue culture cancer cell lines. Because these lines fail to adequately represent the genetic diversity found in the patient population, it is unclear how these findings relate to resistance to tubulin inhibitors in real tumors from patients.

To investigate the differences between receptor negative and receptor positive BC, we measured MT ends (plus tips) dynamics in both interphase and mitotic cells in six BC cell lines. Our measurements showed two main characteristics of the TNBC cells. In interphase cells, the EB1ΔC-2xEGFP speeds were significantly faster for the MDA-MB-231 cell line, with about 6  $\mu\text{m}/\text{min}$  as a median value, than in receptor-positive cells (Matov et al., 2015). The accelerated MT polymerization rates in MDA-MB-231 during interphase likely shortens interphase and accelerates cell cycle progression and mitotic entry, thus increasing their proliferation rates. In all mitotic cells, the EB1 speeds measured at the metaphase plate were around 21  $\mu\text{m}/\text{min}$  (Fig. 1A shows a large mitotic spindle in a receptor-positive BC cell). We did not measure any significant difference in the MT flux (Fig. 2B) in either receptor-negative or receptor-positive cells during metaphase ( $n = 10$ , per cell line), for any of the six cell lines. This indicates that the mechanisms related to differential regulation might be related to the interactions with cytoplasmic molecular motors of the astral and non-kinetochore MTs. Such MT bundles are not tightly anchored, unlike the kinetochore MTs, and their behavior is dependent on the activity of cytoplasmic dynein.

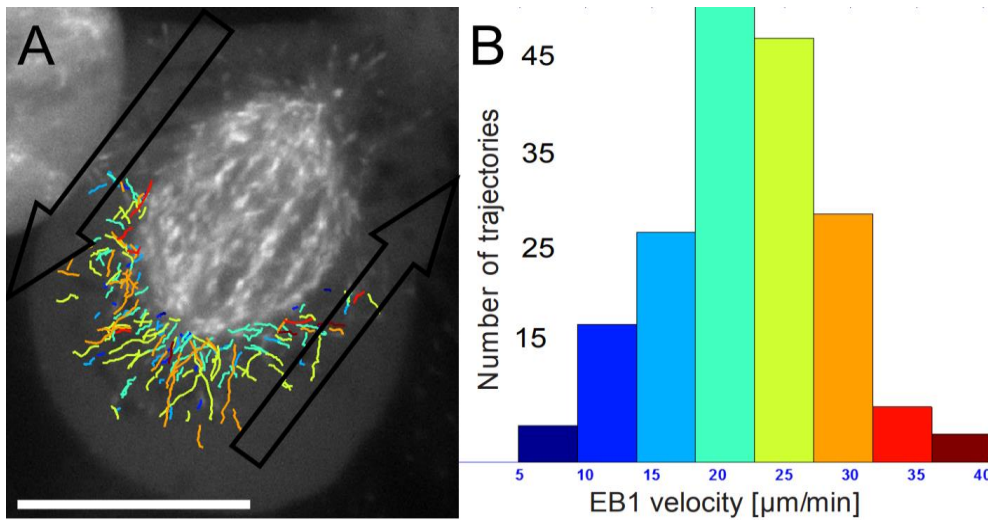


**Figure 1. Mitotic spindle and MT dynamics in a dividing receptor-positive (HCC-1428) BC cell.** (A) MT tips are labeled with EB1 $\Delta$ C-2xEGFP, imaged for a minute (with an acquisition rate of two images per second), and computationally tracked (Yang et al., 2005). The scale bar equals 40  $\mu\text{m}$ . The mitotic spindle exhibits antiparallel MT flux (Matov et al., 2024) and the main two directions are marked with black arrows on the figure. The figure displays, as an overlay, the EB1 trajectories for a specific area of the spindle, namely, only the lower half (below the metaphase plate) and MTs emanating away from the spindle body, the so-called astral MTs. The color-coding represents EB1 speeds and colder colors correspond to lower speeds, and warmer colors correspond to faster speeds. The spindle appeared stationary and EB1 speeds were associated with MT polymerization rates. (B) Histogram of EB1 speed probability density function of the trajectories shown on Fig. 1A. The average speed is  $20.5 \pm 6.2 \mu\text{m}/\text{min}$ . The maximal EB1 speed is about 40  $\mu\text{m}/\text{min}$ . The speed distribution is unimodal and normal.

In this context, what we found remarkable is the rocking pendulum-like motion in many of the mitotic spindles in MDA-MB-231 cells (Fig. 2A and Vid. 1, supplemental data). First, in interphase cells, the MDA-MB-231 cells have the fastest MT polymerization dynamics of about 19  $\mu\text{m}/\text{min}$ . Second, in metaphase, the MDA-MB-231 cells have the largest spindles and, while most of the spindles in the remaining five BC cell lines remain stationary until anaphase, many of them rotate at up to an angle of  $\pm 40^\circ$  (Matov et al., 2015) to the left and right of the polar spindle axis (Vid. 1 and Vid. 2, supplemental data). This rapid rocking motion over an  $80^\circ$  angle is reflected in the measurements for the EB1 velocity (Fig. 2B). Altered MT dynamics endow cancer cells with both survival and migratory advantages (Mitchison, 2012), which can be correlated with drug resistance (Gonçalves et al., 2001). We observed similar rocking motion in dividing cells from the other TNBC cell lines as well.

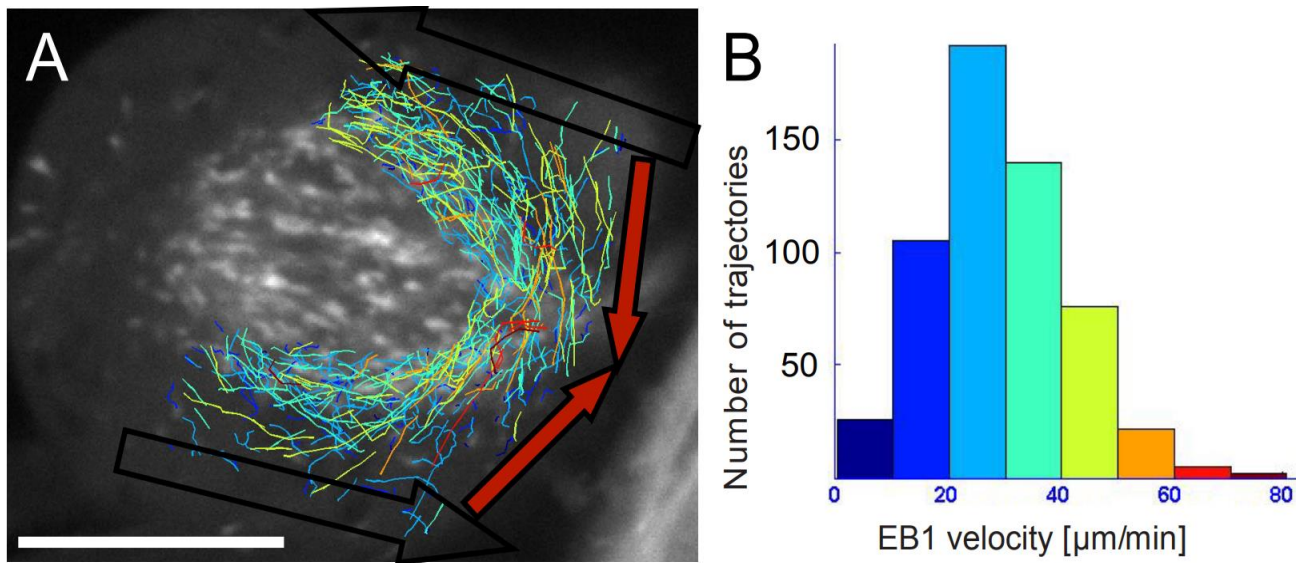


**Figure 2. Mitotic spindle and MT dynamics in a dividing receptor-negative (MBA-MD-231) BC cell.** (A) MT tips are labeled with EB1ΔC-2xEGFP, imaged for a minute (with an acquisition rate of two images per second), and computationally tracked (Yang et al., 2005). The scale bar equals 40 μm. The mitotic spindle exhibits antiparallel MT flux (Matov et al., 2024) and the main two directions are marked with black arrows on the figure. In addition, the spindle exhibits rapid rotational motions and rocks to the left and to the right; the directions of motion of the spindle are marked with red arrows. The figure displays, as an overlay, the EB1 trajectories for a specific area of the spindle, namely, only the right half (to the right of the metaphase plate) and MTs emanating away from the spindle body, the so-called astral MTs. The color-coding represents EB1 speeds and colder colors correspond to lower speeds, and warmer colors correspond to faster speeds. The EB1 speeds were associated with the contribution of both MT polymerization rates and spindle rocking. Because of the extensive motion of the spindle, part of it is obscured by the trajectories overlaid on the image. To observe the rocking motions in the spindle, please see Vid.1 in the supplemental data. (B) Histogram of EB1 speed probability density function of the trajectories shown on Fig. 1A. The average speed is  $29.7 \pm 12.1$  μm/min. The maximal EB1 speed is about 80 μm/min. The speed distribution is unimodal and skewed with a few very fast moving EB1 comets.

## MICROTUBULE REGULATION

There are about 70 MT-associated proteins (MAPs) which regulate various stages of MT homeostasis (Lyle et al., 2009a; Lyle et al., 2009b). Variations in these genes' expression levels have been linked to whether or not a tubulin inhibitor is able to kill the cancer cells (Albrethsen et al., 2014; Berges et al., 2014; Devred et al., 2008; Le Grand et al., 2014; Li et al., 2014; Malesinski et al., 2015; O'Rourke et al., 2014; Thomas et al., 2015; Xie et al., 2015). There are also about 80 proteins at the kinetochore during cell division (Musacchio and Salmon, 2007). Of all solid tumors, BC is the disease with the highest number of tubulin inhibitors approved, consisting of seven stabilizing and destabilizing MT-targeting drugs, suggesting there is variability in patient response. It is unclear whether tubulin inhibitors kill mitotic or interphase cells. It is likely that mitosis is not the target (Field et al., 2014; Kitagawa, 2011; Komlodi-

Pasztor et al., 2011; Komlodi-Pasztor et al., 2012; Komlodi-Pasztor et al., 2013; Mitchison, 2012; Ogden et al., 2013; Weaver, 2015; Wissing et al., 2013) and that the mechanisms by which tubulin inhibitors kill cancer cells in interphase are either absent in tissue culture or masked by the high proliferation rates in a Petri dish. Recently developed compounds (which bind to MT plus ends) designed to induce mitotic arrest (Kapoor et al., 2000) have failed in clinical trials. Drugs like paclitaxel and eribulin (Smith et al., 2010) induce lower mitotic arrest than ispinesib, which failed clinical trials (Dumontet and Jordan, 2010), further highlighting our gap in knowledge in this matter (Topham et al., 2015). These data suggest that, rather than mitotic arrest, a different mechanism, coupled to MT binding in interphase cells, might be essential for the antitumor effect *in vivo* (Zhang et al., 2015). In interphase, a very interesting mechanistic question relates to the ability of different drugs binding to the same site to affect dynamics differentially (Azarenko et al., 2014; Dumontet et al., 2009; Jordan and Wilson, 2004; Kamath et al., 2014; LaPointe et al., 2013; Ngan et al., 2000; Okouneva et al., 2003; Risinger et al., 2014).

There are four canonical parameters describing MT dynamics: MT growth speed, MT shortening speed, catastrophe frequency (which happens when a growing MT switches to a phase of shortening – it equals one over the time a MT spends growing) and rescue frequency (oppositely, this parameters relates to an event when a shortening MT switches to a

phase of growth – it equals one over the time a MT spends shrinking) (Fig. 3, adapted from (Cassimeris et al., 1988)).

As a fifth parameter has commonly been accepted the time of pausing, i.e., the time a MT spends neither growing, nor shortening. In a scenario in which we include pausing as a third MT state besides

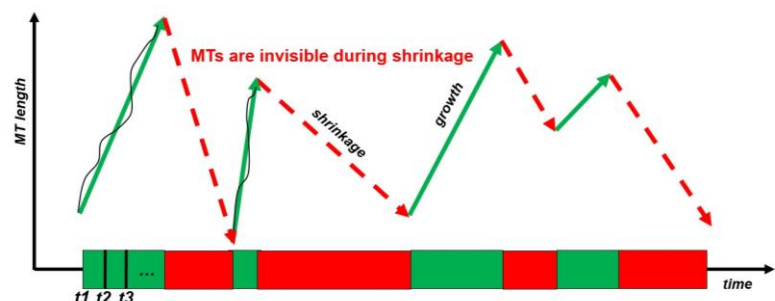


**Figure 3. Evolution of a MT length in time.** Using labeled EB1 proteins, we can directly measure only two of the MT dynamics parameters, MT growth speed and times. Since there is no molecular marker for MT pausing nor MT depolymerization (i.e., one cannot visualize the MTs during these stages), we infer computationally the remaining parameters by assigning multiple visible MT growth tracks to the same trajectory, as depicted in the figure (adapted from (Cassimeris et al., 1988)). Every switch from one phase to another, and changes in the behavior during these phases, is regulated by the genes listed in Table 1.



growth and shortening, there will be additional transitional frequencies parameters back and forth growth-to-pause as well as back and forth shortening-to-pause. Table 1 provides examples of regulators of concrete aspects of MT behavior (Holmfeldt et al., 2009; Sousa et al., 2007). Functional redundancy between specific assembly factors in the chromatin pathway suggest that proteins/pathways commonly viewed as essential may not have unique function, which is important in our quest to target the mitotic spindle in cancer.

Parameter name	MT-regulating proteins	Drug resistance /sensitivity	MT polymerization/ depolymerization activity
Growth speed	chTOG MAP4 TPX2 MAP2 CLIP170	chTOG MAP4 TPX2 MAP2 CLIP170	The rate at which MTs add new dimers, i.e., polymerize
Shrink speed	KIF2C KIF18B TPX2	KIF2C TPX2	The rate at which MTs remove dimers, i.e., depolymerize
Pause times	CLASP VHL	VHL	The time MTs spend stalled, i.e., neither growing nor shortening
Catastrophe frequency	KIF2C Op18 Katanin	KIF2C Op18	Frequency of switch from MT growth to shortening
Rescue frequency	CLASP Tau Katanin	Tau	Frequency of switch from MT shortening to growth

**Table 1. Partial list of dynamics parameters (Matov et al., 2010).** Every aspect of MT dynamicity in living cells is controlled (Bowne-Anderson et al., 2015) by multiple MT-related genes (Lyle et al., 2009a; Lyle et al., 2009b), such as Op18 and XMAP2, whose up- or down-regulation is at the same time linked to resistance to paclitaxel (Inoue and Salmon, 1995; Lyle et al., 2009a; Lyle et al., 2009b; Xie et al., 2015). The full lists of tubulin inhibitors and MT parameters are longer and the regulation is more complex.

## INTERPHASE IN BREAST CANCER CELLS

The cell spends most of its life in interphase. During this time, the MTs are radially stretched from the nucleus toward the cells edge. Linear motion of proteins on MTs during interphase is common in all eukaryotic cells, such as MT plus-end-directed trafficking of proteins or any cargo transported on MTs. Computational analysis of this motion will allow secondary screening of novel tubulin inhibitors or targeted therapies affecting MT-associated proteins. In this context, we performed computational analysis of four BC cells lines before and after the addition of six tubulin inhibitors, three stabilizers and three destabilizers (Table 2). Because tubulin inhibitors are used in the treatment of multiple solid tumors and it is our view that more of them will be approved to treat a variety of tumors of epithelial origin, such as prostate cancer (PCa) and colorectal cancer, we envisaged testing FDA-approved and clinically used MT-stabilizing drugs, such as the taxanes, paclitaxel and docetaxel, as well as some of the MT-destabilizing drugs, such as the vinca alkaloids, vinblastine and vincristine. In addition, we included in our screen

ixabepilone, another MT stabilizer used to treat breast tumors resistant to taxanes (Puhalla and Brufsky, 2008), and eribulin, a MT destabilizer that acts at growing MT ends by a distinct mechanism (Smith et al., 2010). To test different concentrations of these drugs, we performed a pilot study on a panel of five breast cell lines (four BC cell lines and one cell line from normal breast epithelial cells) and treated them with the six tubulin inhibitors. The four BC cell lines we used represented common BC molecular types – Hs578-T (receptor negative), MDA-MB-231 (receptor negative), MCF-7 (estrogen receptor-positive), SKBR3 (human epidermal growth factor receptor 2 (HER2) overexpressing) as well as the normal breast epithelium cells, MCF10A (Matov, 2024a). We performed titration experiments ranging from 0.1 nM to 100 nM concentrations and established that very low drug concentrations of 0.5 nM for MT-stabilizers and 0.1 nM for MT-destabilizers (which have higher potency) allow the cells to remain viable for several days (over a week) after treatment. Because the focus of our analysis is to identify a subset of MT parameters differentially affected by the MT-targeting drugs, higher concentrations, which collapse the cytoskeleton within hours of treatment, will be inappropriate and of questionable translational value considering the pharmacokinetics of many of these drugs in the body (Zasadil et al., 2014).

Our analysis showed that the receptor-negative Hs578-T cells were most susceptible to treatment with paclitaxel (see Table 2, highlighted in red - changes in the values of 10 MT parameters after drug treatment were statistically significant) and ixabepilone (Table 2, highlighted in red - changes in the values of nine MT parameters after drug treatment were statistically significant). Oppositely, according to our measurements, the receptor-negative MDA-MB-231 cells were resistant to all six drugs. The estrogen receptor-positive MCF-7 cells were susceptible to treatment with paclitaxel (Table 2, highlighted in red - changes in the values of nine MT parameters after drug treatment were statistically significant) only. The HER2 overexpressing SKBR3 cells were most susceptible to treatment with ixabepilone (Table 2, highlighted in red - changes in the values of eight MT parameters after drug treatment were statistically significant) and a vinca alkaloid, vinorelbine (Table 2, highlighted in red - changes in the values of eight

MT parameters after drug treatment were statistically significant). Overall, the study showed that there is a variability in drug resistance between TNBC cells and provided a rational for the selection of chemotherapy in the HER2 overexpression setting. According to our computational tracking analysis (Matov et al., 2010), ixabepilone (Goodin, 2008a), a semi-synthetic analog of epothilone B (Goodin, 2008b) would be the most efficient drug to treat the SKBR3 (Fogh et al., 1977) cells. The implications resulting from this determination is that ixabepilone (and vinorelbine) could be used as first line of chemotherapy of HER2 overexpressing breast tumors and also, in some cases, of TNBC tumors. This selection would spare the patients genetically predisposed to not respond to the taxanes the toxicity. A similar conclusion we make also regarding the treatment of the most resistant cells, MDA-MB-231, for which ixabepilone (see Table 2, changes in the values of four MT parameters after drug treatment were statistically significant) and vinorelbine (Table 2, changes in the values of three MT parameters after drug treatment were statistically significant) affected more parameters, and not paclitaxel – approved as a first line of chemotherapy in metastatic BC. In the case of MDA-MB-231 cells, only up to four MT parameters were significantly affected, which suggests a limited impact of treatment with tubulin inhibitors.

Taken together, the results suggest that an assay based on the analysis of living patient-derived cells may offer improvements to the approach established in the current standard of care. It suggests a data-driven algorithm for the identification of efficacious regimens. It also provides an approach for the selection of off-label tubulin inhibitors, which in some cases induce long lasting remission even in very advanced disease stages (Linn et al., 1994). We envisage a system in place, which utilizes pairs of patient normal tissue cells and neoplastic tissue cells for which cytoskeletal reorganization in disease is assessed *ex vivo*. This way, like in a game of Tetris, drugs may be selected for their ability of reversing the full spectrum of disease-induced changes in MT dynamics in anticipation of a maximal treatment efficacy. Our approach might be impactful beyond BC, also in the treatment of other solid tumors. Currently, tubulin inhibitors are not approved for the treatment of many tumors of epithelial origin based on clinical trials, which

require the vast majority of patients to respond to treatment, while in some cancers the response is limited to a fraction of the patients – however, some patients, even if a few, do respond.

	Growth Speeds $\mu\text{m}/\text{min}$	Pause Speeds $\mu\text{m}/\text{min}$	Growth Times $\text{second}$	Pause Times $\text{second}$	Growth Segm. Speeds $\mu\text{m}/\text{min}$	# Pause Growth Segm. A.U.	% T. in Pau. A.U.	Growth Segment Times $\text{second}$	Shrink Speeds $\mu\text{m}/\text{min}$	Shrink Times $\text{second}$	Prob MT Switches to Shrink A.U.	% Time Spend in Shrink A.U.
Hs578-T	11.21	4.53	7.32	11.44	7.02	1.38	43	32.55	8.07	16.08	17.70	13.26
Hs578-T PTX	12.39*	5.28*	6.99*	10.53*	7.77	1.30*	41	28.99*	9.84*	16.69*	26.53*	23.30*
Hs578-T DTX	10.68	4.41	7.80	10.40	6.79	1.36	41	32.32	8.61	16.15	30.81	23.73
Hs578-T iX	15.35*	6.86*	7.78*	9.96	10.18	1.35	40*	30.43*	12.82*	16.64*	29.23*	25.77*
Hs578-T ER	10.72	4.48	7.29	11.01	6.94	1.42	44	31.65	8.84	15.66	27.98	21.99
Hs578-T VNL	12.92*	5.22	6.72*	11.48	8.11	1.41	46*	31.24	9.79*	15.70	26.01*	21.28*
Hs578-T VNC	12.08	4.74	7.16	11.38	7.17	1.37	44	31.18	9.78	15.59	30.46	24.44
MDA231	15.83	7.84	6.10	10.30	10.24	1.27	46	25.64	14.47	16.94	44.16	48.02
MDA231 PTX	16.29	7.42	6.39	10.41	10.42	1.32*	47*	27.12	13.66	17.23	43.34	49.15
MDA231 DTX	9.59	4.24	7.99	11.09	6.43	1.33	41	31.57	8.11	15.90	34.66	27.77
MDA231 iX	19.35*	8.99*	6.29	10.06	12.19	1.26	47*	25.92	16.43*	16.87	44.87	50.32
MDA231 ER	15.17	6.33	5.72	11.16	8.55	1.22	49	25.63	12.88	17.26	43.73	48.32
MDA231 VNL	19.74*	8.75	5.86	9.91	12.42	1.29	45	25.50	16.66*	17.10	36.43*	40.76
MDA231 VNC	9.22	3.99	7.05	10.85	5.96	1.32	42	29.63	6.87	15.95	30.60	26.48
MCF-7	12.54	5.52	7.55	11.14	8.09	1.32	41	31.36	9.69	15.85	29.63	22.72
MCF-7 PTX	10.19*	4.42*	7.42	10.46*	6.95*	1.28*	42	28.78*	7.25*	16.53*	34.58	30.35*
MCF-7 DTX	9.59	4.24	7.99	11.09	6.43	1.33	41	31.57	8.11	15.90	34.66	27.77
MCF-7 iX	12.52	5.57	8.05*	10.39	8.54	1.30	41	30.16	9.68	16.06	33.96	27.17
MCF-7 ER	10.33	4.55	7.37	10.81	6.88	1.32	43	30.44	7.91	16.90	31.75	27.33
MCF-7 VNL	12.57	5.36	7.03*	10.68	8.22	1.33	43	29.67	9.02	16.34	30.52	25.71
MCF-7 VNC	9.22	3.99	7.05	10.85	5.96	1.32	42	29.63	6.87	15.95	35.06	26.48

SKBR3	11.30	4.95	6.06	12.20	6.69	1.23	49	27.89	8.59	15.62	36.3	29.40
SKBR3 PTX	11.88	5.17*	6.05	11.62	7.31*	1.14*	48	25.41*	8.78	16.51	42.3*	13.51*
SKBR3 DTX	12.18	5.50	5.79	11.76	7.45	1.22	51	26.4	10.22	16.63	49.45	53.33
SKBR3 iX	16.14*	7.28*	5.91	11.55	9.96	1.18*	49	25.85*	13.27*	16.35*	50.66*	51.95*
SKBR3 ER	12.69	5.42	5.78	12.40	7.63	1.24	50	27.11	10.38	16.64	48.23	48.66
SKBR3 VNL	15.01*	6.84*	5.48*	11.89	9.53	1.15*	50*	24.97	11.85*	16.14	46.86*	49.49*
SKBR3 VNC	11.68	5.24	5.41	11.91	7.21	1.19	51	25.10	10.72	16.02	47.50	51.85

**Table 2. Quantitative measurement of MT dynamics in four BC cell lines treated with six tubulin inhibitors.** Computational analysis of MT dynamics performed using ClusterTrack (Matov et al., 2010). The cell lines consist of HER2 overexpressing (SKBR3), triple-negative (MDA-231), ER+ cells (MCF7) and ER- cells (Hs578), the four most common types of breast cancers exhibited by metastatic patients. The MT inhibitors we used were ixabepilone (iX), docetaxel (DTX), paclitaxel (PTX) (MT stabilizers; treatment at concentration 0.5 nM), eribulin (ER), vinorelbine (VNL), vincristine (VNC) (MT destabilizers; treatment at concentration 0.1 nM). For each of the 28 conditions, 20 movies were analyzed. Each movie consists of 120 frames taken 0.5 seconds apart. Asterisks\* denote statistically significant shifts in MT parameter values, which were calculated on per-cell basis as well as at the level of individual microtubules. Observe the nonlinear effects of the drugs, as it is established that a high dose of paclitaxel stabilizes MTs, while, as we measured here, a low dose systematically increased MT polymerization rates in all cells but MDA-MB-231. The study also provided a rationale for the selection of chemotherapy in the HER2+ setting, where, according to our computational analysis, ixabepilone would be the most efficient drug to treat the SKBR3 cells.

The 12 MT dynamics parameters (Matov et al., 2010) are as follows: (1) MT polymerization rates (growth speeds), (2) MT dynamics during trajectory gaps, when the EB1ΔC-2xEGFP molecular marker is not visible (pause/gap speeds), (3) MT polymerization periods (growth times), (4) periods of MT pausing and trajectory gaps, when the EB1ΔC-2xEGFP molecular marker is not visible (pause/gap times), (5) MT polymerization rates over multiple trajectories interrupted by periods when the EB1-EGFP molecular marker is not visible (growth segment speeds), (6) number of periods when the EB1ΔC-2xEGFP molecular marker is not visible within MT growth segments (number of pause/gaps per growth segment), (7) percent of time MTs spend pausing within the growth segments (percent time in pause/gap), (8) periods of MT polymerization rates over multiple trajectories interrupted by periods when the EB1ΔC-2xEGFP molecular marker is not visible (growth segment times), (9) MT depolymerization rates (shrink/shortening speeds), (10) MT depolymerization periods (shrink/shortening times), (11) probability of MTs to switch from polymerization to depolymerization, i.e., to undergo catastrophe, at the end of a MT growth segment, (12) percent of time MTs spend depolymerizing within composite MT trajectories (percent time in shrink/shortening).

The rates of polymerization, depolymerization, and pausing motion are measured in micrometers per minutes. The duration of the periods of polymerization, depolymerization, and pausing are measured in seconds. The remaining parameters are measured in arbitrary units.

## MITOSIS IN PATIENT CELLS

Even if the overall regulation is a complex process, three nucleation/stabilization factors (Groen et al., 2009), TPX2,  $\gamma$ -tubulin and XMAP215/chTOG are required for MT polymerization and bipolar spindle assembly around chromatin beads in an *in vitro* system. Depletion of TPX2 was partially rescued by inhibiting MCAK/KIF2C or by adding EB1 or by adding XMAP215/chTOG. Depletion of

XMAP215/chTOG or depletion of  $\gamma$ -tubulin was partially rescued by adding XMAP215/chTOG, but not by adding other factors. This demonstrates that for the functioning of the spindle is required a minimal level of multiple MT regulators. In this context, aberrant MT dynamics in cancer can be exploited by targeting the specific genes responsible for generating them. It is conceivable that (i) depletion of multiple MT regulators will reverse resistance and sensitize cancer cells to tubulin inhibitors and (ii) further depletion will eventually make the cells apoptotic. Differential expression of MT regulating genes affects specific parameters of MT dynamics, thus determining the sensitivity to treatment. Combining personalized tubulin inhibitor chemotherapy and customized list of cancer-specific targets within the MT-regulating genes based on the techniques described in the specific aims might offer therapeutic plans resulting in both low toxicity and low disease relapse rates.

In previous work (Harkcom et al., 2014), we measured an increase in MT dynamicity in a BC MCF-7 cell line after treatment with Nicotinamide adenine dinucleotide (NAD<sup>+</sup>), an endogenous small molecule that has effects on diverse processes, including obesity, lifespan, and cancer, by tracking the motion of the MT end-binding protein EB1. The prototypical end-binding protein EB1 recognizes conformational changes in tubulin dimers and binds specifically to MT tips during polymerization (growth). To visualize MT tips in BC cells, we induce them to express the MT plus-end marker EB1 $\Delta$ C-2xEGFP by lentivirus transduction. MT polymerization dynamics as a function of drug concentration will be analyzed by lentivirus-mediated low level expression of EB1 $\Delta$ C-2xEGFP, a marker of growing MT plus ends that does not interfere with endogenous EB1 binding partners (Gierke and Wittmann, 2012). When EB1 is fused to EGFP, the EGFP-EB1 dimers at the MT tip form a fluorescent comet which serves as a molecular marker for the direct visualization of MT polymerization dynamics using time-lapse fluorescence microscopy.

Polo-like kinase 1 (PLK1) is the principle member of the serine/threonine kinase family (Chiappa et al., 2022) and is overexpressed in TNBC (Ueda et al., 2019). PLK1 inhibition affects MT dynamics by

suppressing polymerization rates (Brennan et al., 2008), which leads to spindle shortening. This effect on the regulation of mitosis can be reversed by the addition of paclitaxel (Brennan et al., 2008), which stabilizes MTs – in this scenario, at their minus ends. When MT plus-end-directed motors are suppressed (Matov et al., 2024), MT sliding toward the spindle pole maintains MT flux, likely driven by cytoplasmic dynein (Gudimchuk and McIntosh, 2021), which suggests the use of combination therapies. One avenue to overcome resistance to tubulin inhibitors is to use a combination therapy with PLK1 inhibitors (Su et al., 2022).

The lack of methods for visualizing MT minus ends has been an obstacle to the precise analysis of MT depolymerization (Matov et al., 2010). It would be informative to be able to quantify the dynamics of human MTs while they depolymerize, at either their plus or minus ends, by modifying proteins like Dam1 (Gardner and Odde, 2008), Ska1 (Ye and Maresca, 2013), NOD (Cane et al., 2013) or DDA3 (Jiang et al., 2012). Such measurements would allow to determine the secondary molecular mechanisms activated in drug-treated cancer cells leading to the development of resistance and, thus, inform therapy and select combination therapy to which the disease would respond.

To translate such results to clinically-relevant models, one can transfer this technology to BC organoids (Sachs et al., 2018). Classification of trajectories can be accomplished by mimicking patient treatment in the organoids and accessing results of measurements of patient tumors which show if the (i) tumors recede, i.e., respond to treatment or (ii) grow/show no change, i.e., exhibit drug resistance. Additionally, one can expect to be able to further sub-classify the resistant signatures based on the mechanism behind it. These steps will be repeated and novel significant MT signatures will be recorded as treatment progresses, which will allow for the accumulation of large signature populations, which will then allow for statistical analyses. Further, because organoid cultures are susceptible to molecular manipulations (Koo et al., 2013),

one can reduce MT regulators expression by shRNA or CRISPR and ask whether this counteracts drug resistance and restores normal MT dynamics by mRNA-based drugs in a physiologically relevant system.

We conducted a preliminary investigation in colon cancer organoids (Fig. 4A), for which the organoid culture is better established (van de Wetering et al., 2015). Our measurements (Fig. 4B) indicate that these patient organoid cells have MTs polymerizing with rates characteristics for chromosomal instability (Ertych et al., 2014) and significantly faster than for the commonly utilized colon cancer cell lines when cultured in a monolayer, highlighting the importance of physiological 3D organoid model systems for the fidelity of the measurements. The cells in the organoid form a lumen and to the left is visible a mitotic cell (Fig. 4A). The mitotic spindle rotates rapidly (Vid. 3, supplemental data) similarly to the spindles in MDA-MB-231 cells and this suggests that this patient could be resistant to therapy. We observe and measure strong lateral rotation in the spindle (red arrows on Fig. 4A), which results in fast EB1 speeds (Fig. 4B and Vid. 4, supplemental data).

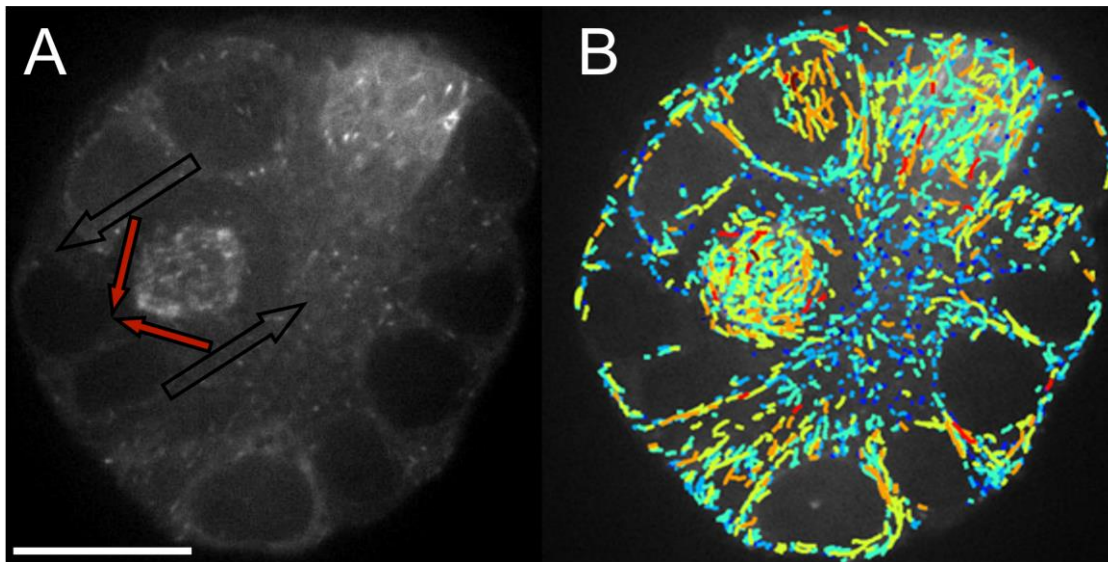


**Figure 4 Measurements of MT signatures in patient-derived cancer organoids.** (A) EB1 $\Delta$ C-2xEGFP in stably expressed in colon cancer organoids (scale bar equals 70  $\mu$ m). (B) Computer-generated MT growth tracks (Yang et al., 2005). The color-coding represents EB1 speeds and colder colors correspond to lower speeds, and warmer colors correspond to faster speeds. Note the mitotic spindle of a dividing cancer cell on the left side of the image. The average growth rate in this specimen is 19  $\mu$ m/min, which is significantly faster compared with colon cancer cells cultured in a 2D monolayer, highlighting the importance of physiological 3D organoid model systems for the fidelity of the measurements.



## INTERPHASE IN PATIENT CELLS

We expressed fluorescently tagged MT markers by using lentivirus-mediated transduction and our MT dynamics analysis indicates differences between different PCa organoids (Fig. 5). Analysis of available RNA-Seq. data shows intriguing differences in expression levels of MT regulators, and EB1 comet tracking indicates a correlation of decreased MT polymerization rates with increased Op18 (Fig. 5A) and KIF2C expression, providing an indication of a physiological mechanism of resistance in patient tumors. Organoid PCa1 shows high levels of MT destabilizing factors, including Op18 (Matov et al., 2016) and had not undergone docetaxel chemotherapy (Gao et al., 2014), to which the tumor would likely have been resistant. We predict that we will find similar high Op18 expressing cases in taxane resistant organoids established from BC patient cells. We could define a subtype of Op18 expressing tumors, and directly test how such patient cells and MT dynamics respond to different drugs compared with other organoids with low Op18 expression level. Patient organoids overexpressing the tubulin-sequestering protein Op18 may be resistant to elevated taxane concentrations, but may still be sensitive to other tubulin inhibitors. This outcome would be clinically relevant and suggest a possible novel therapeutic strategy.

In particular, the approach can be applied for the *ex vivo* evaluation of the efficacy of mRNA-based drugs. The inset on Fig. 5A shows that the EB1 speeds in organoid PCa1 form a multi-modal distribution (the four peaks are marked with red lines). The reason behind this type of distribution may be that the activity of different genes regulating MT polymerization (Table 1), for example the expression levels of chTOG, MAP2, and CLIP170, lead to the different modes in the speed distribution. By knockdown or reconstitution of each of these genes and consequent analysis of the derivative cultures we could delineate their precise contribution to the abnormal behavior of the MT cytoskeleton in disease. This approach can, thus, be utilized as a strategy for the selection of novel targets in the context of overcoming resistance to therapy in BC. Besides sensitizing drugs, our strategy could be utilized for the identification of putative targets within the MT transcriptome.

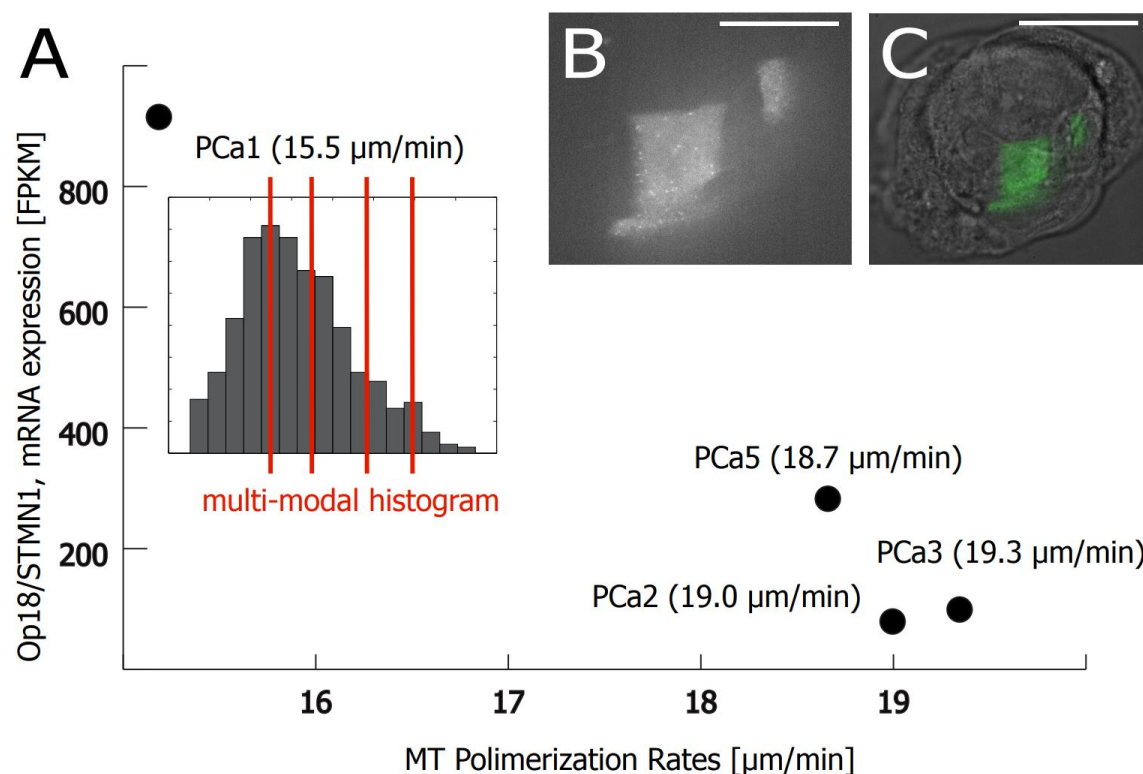


**Figure 5 . RNA-Seq. data from the MSKCC mCRPC organoids showing high expression of Op18 in PCa1 correlates with attenuated MT polymerization rates measured by motion analysis of EB1 $\Delta$ C-2xEGFP comets. (A) Numbers in brackets show preliminary MT growth rates from a limited number of cells measured (Yang et al., 2005); inset shows the histogram of MT growth rates in PCa1 with a mean value of 15.5  $\mu\text{m}/\text{min}$ ; multi-modal distribution may be resulting from contributions of four or five genes which regulate MT growth. This analysis can be used to generate a shortlist of candidate genes involved in the regulation of MT dynamics for targeted therapy, such RNA therapy, to sensitize resistant tumor cells. (B) Spinning disc confocal microscopy image (scale bar equals 50  $\mu\text{m}$ ) of a patient organoid with cells expressing EB1 $\Delta$ C-2xEGFP a day after radical prostatectomy, observe only three cells in the round organoid are transduced. (C) The same organoid as in (B), the three EB1 $\Delta$ C-2xEGFP expressing cells are pseudo-colored in green and overlaid with the organoid imaged in transmitted light (scale bar equals 70  $\mu\text{m}$ ).**

## CONCLUSIONS

The treatment of advanced BC is hampered by the emergence of drug resistance. The first four lines of chemotherapy consist of “one size fits all” regimens, yet BC is molecularly a heterogeneous disease. We describe an approach for drug selection in BC, which is based on the computational analysis of live-cell microscopy of patient-derived cells *ex vivo*. It reveals differences in the response to tubulin inhibitors even in TNBC, for which the resistance to taxanes is not universal. Differences in the ability of drugs to kill cancer cells stem from the level of drug-target engagement, which cannot necessarily be predicted by genetic sequencing alone. In this context, quantitative live-cell microscopy may aid anticipating whether a compound has the ability to affect the desired molecular target.

## **MATERIALS AND METHODS**

### **Image Analysis**

All image analysis programs for detection and tracking of comets, and graphical representation of the results were developed in MATLAB (Mathworks, MA) and C/C++. The EB1 comet analysis method ClusterTrack used is described and validated in (Matov et al., 2010). The computer code is available for download at: <https://www.github.com/amatov/ClusterTrackTubuline>.

### **Cell Culture**

MT polymerization dynamics was visualized by lentivirus-mediated low level expression of EB1 $\Delta$ C-2xEGFP, a marker of growing MT plus-ends that does not interfere with endogenous EB1 binding partners. We expressed fluorescently tagged MT markers in the organoids by using lentivirus-mediated transduction (Fig. 5B) and had best results infecting small organoids in an early exponential growth phase. To optimize imaging conditions, blasticidin selection was tuned such that only 20-30% of organoid cells are GFP-labeled (Fig. 5C). This way, we achieved better contrast of imaging EB1 and MT dynamics.

### **Microscopy Imaging**

We imaged EB1 $\Delta$ C-2xEGFP-expressing organoids (Koo et al., 2013) by time-lapse spinning disk confocal microscopy using a long working distance 60x magnification water immersion 1.4 NA objective and a 100x magnification oil immersion 1.45 NA objective for all cultured cells. We acquired images at half a second intervals for a minute to collect datasets without photobleaching (Gierke and Wittmann, 2012).

### **Ethics Declaration**

Approval of tissue requests #14-04 and #16-5 to the UCSF Cancer Center Tissue Core and the Genitourinary Oncology Program was given.

## **ACKNOWLEDGEMENTS**

I thank Julia Rohrberg for giving me the opportunity to collect image datasets for this manuscript while I was imaging cells for (Rohrberg et al., 2020), Torsten Wittmann, Tom Maresca and Aaron Groen for discussing cytoskeleton regulation with me, and Johan de Rooij for labeling the colon cancer organoid with EB1 $\Delta$ C-2xEGFP. The computational results in Table 2 were obtained by Jesús Acevedo, a summer exchange student, and Daniel Bidikov, a summer high-school student, while I was training them in using ClusterTrack (Matov et al., 2010) on image datasets I obtained with the help of Benet Pera. I am grateful to the Genitourinary Tissue Utilization committee and the Genitourinary and Prostate SPORE Tissue Cores at the UCSF Cancer Center for the approval of my tissue requests #14-04 and #16-5 and the Stand Up To Cancer / Prostate Cancer Foundation (SU2C/PCF) West Coast Dream Team (WCDT).

## **SUPPLEMENTARY MATERIALS**

Video 1 – Time-lapse movie of a rocking mitotic spindle of a MDA-MB-231 cell with labeled EB1 comets (example #1). <https://vimeo.com/382125072/bce76f2ef0>

Video 2 – Time-lapse movie of a rocking mitotic spindle of a MDA-MB-231 cell with labeled EB1 comets (example #2). <https://vimeo.com/382256739/ccd8ab1b63>

Video 3 – Time-lapse movie of colorectal organoid with a rocking mitotic spindle with labeled EB1 comets. <https://vimeo.com/995869434/e93d5ae421>

Video 4 – Time-lapse movie of colorectal organoid with tracking of EB1 comets. Different colors are used for the different trajectories. All trajectories are visible only during the periods of MT polymerization and afterwards are removed from the screen to improve visibility. <https://vimeo.com/995872753/173a2843bf>

## REFERENCES

- Albrethsen, J., R.H. Angeletti, S.B. Horwitz, and C.P. Yang. 2014. Proteomics of cancer cell lines resistant to microtubule-stabilizing agents. *Mol Cancer Ther.* 13:260-269.
- Azarenko, O., G. Smiyun, J. Mah, L. Wilson, and M.A. Jordan. 2014. Antiproliferative mechanism of action of the novel taxane cabazitaxel as compared with the parent compound docetaxel in MCF7 breast cancer cells. *Mol Cancer Ther.* 13:2092-2103.
- Berges, R., N. Baeza-Kallee, E. Tabouret, O. Chinot, M. Petit, A. Kruczynski, D. Figarella-Branger, S. Honore, and D. Braguer. 2014. End-binding 1 protein overexpression correlates with glioblastoma progression and sensitizes to Vinca-alkaloids in vitro and in vivo. *Oncotarget.* 5:12769-12787.
- Bowne-Anderson, H., A. Hibbel, and J. Howard. 2015. Regulation of Microtubule Growth and Catastrophe: Unifying Theory and Experiment. *Trends Cell Biol.*
- Brennan, I., A. Matov, G. Danuser, and A. Straight. 2008. Polo-like Kinase Regulation of Anaphase Spindle Elongation. *Molecular biology of the cell.* 19.
- Cane, S., A.A. Ye, S.J. Luks-Morgan, and T.J. Maresca. 2013. Elevated polar ejection forces stabilize kinetochore-microtubule attachments. *The Journal of cell biology.* 200:203-218.
- Cassimeris, L., N.K. Pryer, and E.D. Salmon. 1988. Real-time observations of microtubule dynamic instability in living cells. *J Cell Biol.* 107:2223-2231.
- Chiappa, M., S. Petrella, G. Damia, M. Broggin, F. Guffanti, and F. Ricci. 2022. Present and Future Perspective on PLK1 Inhibition in Cancer Treatment. *Frontiers in oncology.* 12:903016.
- Clevers, H., and E. Bender. 2015. Q&A: Hans Clevers. Banking on organoids. *Nature.* 521:S15.
- Devred, F., P.O. Tsvetkov, P. Barbier, D. Allegro, S.B. Horwitz, A.A. Makarov, and V. Peyrot. 2008. Stathmin/Op18 is a novel mediator of vinblastine activity. *FEBS Lett.* 582:2484-2488.
- Dumontet, C., and M.A. Jordan. 2010. Microtubule-binding agents: a dynamic field of cancer therapeutics. *Nature reviews. Drug discovery.* 9:790-803.
- Dumontet, C., M.A. Jordan, and F.F. Lee. 2009. Ixabepilone: targeting betaIII-tubulin expression in taxane-resistant malignancies. *Mol Cancer Ther.* 8:17-25.
- Ertych, N., A. Stolz, A. Stenzinger, W. Weichert, S. Kaulfuss, P. Burfeind, A. Aigner, L. Wordeman, and H. Bastians. 2014. Increased microtubule assembly rates influence chromosomal instability in colorectal cancer cells. *Nat Cell Biol.* 16:779-791.
- Field, J.J., A. Kanakkanthara, and J.H. Miller. 2014. Microtubule-targeting agents are clinically successful due to both mitotic and interphase impairment of microtubule function. *Bioorg Med Chem.* 22:5050-5059.

- Fogh, J., J.M. Fogh, and T. Orfeo. 1977. One hundred and twenty-seven cultured human tumor cell lines producing tumors in nude mice. *Journal of the National Cancer Institute*. 59:221-226.
- Gao, D., I. Vela, A. Sboner, P.J. Iaquinta, W.R. Karthaus, A. Gopalan, C. Dowling, J.N. Wanjala, E.A. Undvall, V.K. Arora, J. Wongvipat, M. Kossai, S. Ramazanoglu, L.P. Barboza, W. Di, Z. Cao, Q.F. Zhang, I. Sirota, L. Ran, T.Y. MacDonald, H. Beltran, J.M. Mosquera, K.A. Touijer, P.T. Scardino, V.P. Laudone, K.R. Curtis, D.E. Rathkopf, M.J. Morris, D.C. Danila, S.F. Slovin, S.B. Solomon, J.A. Eastham, P. Chi, B. Carver, M.A. Rubin, H.I. Scher, H. Clevers, C.L. Sawyers, and Y. Chen. 2014. Organoid cultures derived from patients with advanced prostate cancer. *Cell*. 159:176-187.
- Gardner, M.K., and D.J. Odde. 2008. Dam1 complexes go it alone on disassembling microtubules. *Nature cell biology*. 10:379-381.
- Giannakakou, P., R. Gussio, E. Nogales, K.H. Downing, D. Zaharevitz, B. Bollbuck, G. Poy, D. Sackett, K.C. Nicolaou, and T. Fojo. 2000. A common pharmacophore for epothilone and taxanes: molecular basis for drug resistance conferred by tubulin mutations in human cancer cells. *Proc Natl Acad Sci U S A*. 97:2904-2909.
- Giannakakou, P., D.L. Sackett, Y.K. Kang, Z. Zhan, J.T. Buters, T. Fojo, and M.S. Poruchynsky. 1997. Paclitaxel-resistant human ovarian cancer cells have mutant beta-tubulins that exhibit impaired paclitaxel-driven polymerization. *J Biol Chem*. 272:17118-17125.
- Gierke, S., and T. Wittmann. 2012. EB1-recruited microtubule +TIP complexes coordinate protrusion dynamics during 3D epithelial remodeling. *Current biology : CB*. 22:753-762.
- Gonçalves, A., D. Braguer, K. Kamath, L. Martello, C. Briand, S. Horwitz, L. Wilson, and M.A. Jordan. 2001. Resistance to Taxol in lung cancer cells associated with increased microtubule dynamics. *Proc Natl Acad Sci U S A*. 98:11737-11742.
- Goodin, S. 2008a. Ixabepilone: a novel microtubule-stabilizing agent for the treatment of metastatic breast cancer. *American journal of health-system pharmacy : AJHP : official journal of the American Society of Health-System Pharmacists*. 65:2017-2026.
- Goodin, S. 2008b. Novel cytotoxic agents: epothilones. *American journal of health-system pharmacy : AJHP : official journal of the American Society of Health-System Pharmacists*. 65:S10-15.
- Groen, A.C., T.J. Maresca, J.C. Gatlin, E.D. Salmon, and T.J. Mitchison. 2009. Functional overlap of microtubule assembly factors in chromatin-promoted spindle assembly. *Mol Biol Cell*. 20:2766-2773.
- Gudimchuk, N.B., and J.R. McIntosh. 2021. Regulation of microtubule dynamics, mechanics and function through the growing tip. *Nature reviews. Molecular cell biology*. 22:777-795.
- Gundersen, G.G., and T.A. Cook. 1999. Microtubules and signal transduction. *Curr Opin Cell Biol*. 11:81-94.

- Haber, M., C.A. Burkhardt, D.L. Regl, J. Madafiglio, M.D. Norris, and S.B. Horwitz. 1995. Altered expression of M beta 2, the class II beta-tubulin isotype, in a murine J774.2 cell line with a high level of taxol resistance. *J Biol Chem.* 270:31269-31275.
- Hanahan, D., and R.A. Weinberg. 2000. The hallmarks of cancer. *Cell.* 100:57-70.
- Hanahan, D., and R.A. Weinberg. 2011. Hallmarks of cancer: the next generation. *Cell.* 144:646-674.
- Harkcom, W.T., A.K. Ghosh, M.S. Sung, A. Matov, K.D. Brown, P. Giannakakou, and S.R. Jaffrey. 2014. NAD<sup>+</sup> and SIRT3 control microtubule dynamics and reduce susceptibility to antimicrotubule agents. *Proc Natl Acad Sci U S A.* 111:E2443-2452.
- Holmfeldt, P., M.E. Sellin, and M. Gullberg. 2009. Predominant regulators of tubulin monomer-polymer partitioning and their implication for cell polarization. *Cellular and molecular life sciences : CMLS.* 66:3263-3276.
- Inoue, S. 1959. Motility of Cilia and the Mechanism of Mitosis. *Reviews of Modern Physics.* 31:402-408.
- Inoue, S., and E.D. Salmon. 1995. Force generation by microtubule assembly/disassembly in mitosis and related movements. *Mol Biol Cell.* 6:1619-1640.
- Jiang, K., G. Toedt, S. Montenegro Gouveia, N.E. Davey, S. Hua, B. van der Vaart, I. Grigoriev, J. Larsen, L.B. Pedersen, K. Bezstarosti, M. Lince-Faria, J. Demmers, M.O. Steinmetz, T.J. Gibson, and A. Akhmanova. 2012. A Proteome-wide screen for mammalian SxIP motif-containing microtubule plus-end tracking proteins. *Current biology : CB.* 22:1800-1807.
- Jordan, M.A., and L. Wilson. 2004. Microtubules as a target for anticancer drugs. *Nature reviews. Cancer.* 4:253-265.
- Kamath, K., G. Smiyun, L. Wilson, and M.A. Jordan. 2014. Mechanisms of inhibition of endothelial cell migration by taxanes. *Cytoskeleton (Hoboken, N.J.).* 71:46-60.
- Kanakkanthara, A., and J.H. Miller. 2012. MicroRNAs: novel mediators of resistance to microtubule-targeting agents. *Cancer Treat Rev.* 39:161-170.
- Kanakkanthara, A., A. Wilmes, A. O'Brate, D. Escuin, A. Chan, A. Gjyzezi, J. Crawford, P. Rawson, B. Kivell, P.T. Northcote, E. Hamel, P. Giannakakou, and J.H. Miller. 2011. Peloruside- and laulimalide-resistant human ovarian carcinoma cells have betaI-tubulin mutations and altered expression of betaII- and betaIII-tubulin isotypes. *Mol Cancer Ther.* 10:1419-1429.
- Kapoor, T.M., T.U. Mayer, M.L. Coughlin, and T.J. Mitchison. 2000. Probing spindle assembly mechanisms with monastrol, a small molecule inhibitor of the mitotic kinesin Eg5. *J. Cell Biol.* 150:975 - 988.
- Kitagawa, K. 2011. Too early to say, "no targeting of mitosis!". *Nat Rev Clin Oncol.* 8:444; author reply 444.
- Komlodi-Pasztor, E., D. Sackett, J. Wilkerson, and T. Fojo. 2011. Mitosis is not a key target of microtubule agents in patient tumors. *Nat Rev Clin Oncol.*

- Komlodi-Pasztor, E., D.L. Sackett, and A.T. Fojo. 2012. Inhibitors Targeting Mitosis: Tales of How Great Drugs against a Promising Target Were Brought Down by a Flawed Rationale. *Clin Cancer Res.* 18:51-63.
- Komlodi-Pasztor, E., D.L. Sackett, and T. Fojo. 2013. Tales of how great drugs were brought down by a flawed rationale--response. *Clin Cancer Res.* 19:1304.
- Koo, B.K., V. Sasselli, and H. Clevers. 2013. Retroviral gene expression control in primary organoid cultures. *Current protocols in stem cell biology.* 27:Unit 5A.6.
- LaPointe, N.E., G. Morfini, S.T. Brady, S.C. Feinstein, L. Wilson, and M.A. Jordan. 2013. Effects of eribulin, vincristine, paclitaxel and ixabepilone on fast axonal transport and kinesin-1 driven microtubule gliding: implications for chemotherapy-induced peripheral neuropathy. *Neurotoxicology.* 37:231-239.
- Le Grand, M., A. Rovini, V. Bourgarel-Rey, S. Honore, S. Bastonero, D. Braguer, and M. Carre. 2014. ROS-mediated EB1 phosphorylation through Akt/GSK3beta pathway: implication in cancer cell response to microtubule-targeting agents. *Oncotarget.* 5:3408-3423.
- Li, X., R. Yao, L. Yue, W. Qiu, W. Qi, S. Liu, Y. Yao, and J. Liang. 2014. FOXM1 mediates resistance to docetaxel in gastric cancer via up-regulating Stathmin. *J Cell Mol Med.* 18:811-823.
- Linn, S.C., G. Giaccone, and H.M. Pinedo. 1994. Complete remission of metastatic colorectal cancer: a pitfall in a multidrug resistance reversal trial. *Lancet.* 343:1648-1649.
- Lyle, K., P. Kumar, and T. Wittmann. 2009a. SnapShot: Microtubule Regulators I. *Cell.* 136:380, 380.e381.
- Lyle, K., P. Kumar, and T. Wittmann. 2009b. SnapShot: Microtubule regulators II. *Cell.* 136:566, 566.e561.
- Maddox, P., A. Straight, P. Coughlin, T.J. Mitchison, and E.D. Salmon. 2003. Direct observation of microtubule dynamics at kinetochores in *Xenopus* extract spindles: implications for spindle mechanics. *J. Cell Biol.* 162:377-382.
- Malesinski, S., P.O. Tsvetkov, A. Kruczynski, V. Peyrot, and F. Devred. 2015. Stathmin potentiates vinflunine and inhibits Paclitaxel activity. *PLoS One.* 10:e0128704.
- Maqbool, M., F. Bekele, and G. Fekadu. 2022. Treatment Strategies Against Triple-Negative Breast Cancer: An Updated Review. *Breast cancer (Dove Medical Press).* 14:15-24.
- Matov, A. 2024a. Computational Analysis of Treatment Resistant Cancer Cells. *medRxiv*:2024.08.29.24312813.
- Matov, A. 2024b. A Real-Time Suite of Biological Cell Image Analysis Software for Computers, Smartphones, and Smart Glasses, Suitable for Resource-Constrained Computing. *arXiv*:2407.15735.
- Matov, A., K. Applegate, P. Kumar, C. Thoma, W. Krek, G. Danuser, and T. Wittmann. 2010. Analysis of microtubule dynamic instability using a plus-end growth marker. *Nature Methods.* 7:761- 768.



- Matov, A., A. Bacconi, and J.C. Gatlin. 2024. Instantaneous Flow Analysis of Contractile Cytoskeletal Structures Affected by the Dysregulation of Kinesin and Tropomyosin Motors. *bioRxiv*:2024.06.28.601275.
- Matov, A., J. de Rooij, J.C. Gatlin, J. Rohrberg, N. Ahmad, R. Aggarwal, J. Simko, A. Goga, C.J. Ryan, and T. Wittmann. 2016. Investigating microtubule growth dynamics in patient-derived metastatic prostate cancer cells. *Cancer Research*. 76:243.
- Matov, A., J. Rohrberg, A. Goga, and T. Wittmann. 2015. Investigating Microtubule Growth Dynamics and Spindle Positioning Regulation in Breast Cancer Cells *Molecular biology of the cell*. 26.
- Mitchison, T., and M. Kirschner. 1984. Dynamic Instability of Microtubule Growth. *Nature*. 312:237-242.
- Mitchison, T.J. 2012. The proliferation rate paradox in antimitotic chemotherapy. *Mol Biol Cell*. 23:1-6.
- Musacchio, A., and E.D. Salmon. 2007. The spindle-assembly checkpoint in space and time. *Nature reviews. Molecular cell biology*. 8:379-393.
- Ngan, V.K., K. Bellman, D. Panda, B.T. Hill, M.A. Jordan, and L. Wilson. 2000. Novel actions of the antitumor drugs vinflunine and vinorelbine on microtubules. *Cancer Res*. 60:5045-5051.
- O'Rourke, B., C.P. Yang, D. Sharp, and S.B. Horwitz. 2014. Eribulin disrupts EB1-microtubule plus-tip complex formation. *Cell cycle (Georgetown, Tex.)*. 13:3218-3221.
- Ogden, A., P.C. Rida, M.D. Reid, and R. Aneja. 2013. Interphase microtubules: chief casualties in the war on cancer? *Drug Discov Today*. 19:824-829.
- Okouneva, T., B.T. Hill, L. Wilson, and M.A. Jordan. 2003. The effects of vinflunine, vinorelbine, and vinblastine on centromere dynamics. *Mol Cancer Ther*. 2:427-436.
- Orr, G.A., P. Verdier-Pinard, H. McDaid, and S.B. Horwitz. 2003. Mechanisms of Taxol resistance related to microtubules. *Oncogene*. 22:7280-7295.
- Puhalla, S., and A. Brufsky. 2008. Ixabepilone: a new chemotherapeutic option for refractory metastatic breast cancer. *Biologics : targets & therapy*. 2:505-515.
- Ranganathan, S., C.A. Benetatos, P.J. Colarusso, D.W. Dexter, and G.R. Hudes. 1998. Altered beta-tubulin isotype expression in paclitaxel-resistant human prostate carcinoma cells. *British journal of cancer*. 77:562-566.
- Risinger, A.L., S.M. Riffle, M. Lopus, M.A. Jordan, L. Wilson, and S.L. Mooberry. 2014. The taccalonolides and paclitaxel cause distinct effects on microtubule dynamics and aster formation. *Molecular cancer*. 13:41.
- Robert, J. 1999. Multidrug resistance in oncology: diagnostic and therapeutic approaches. *European journal of clinical investigation*. 29:536-545.

- Rohrberg, J., D. Van de Mark, M. Amouzgar, J.V. Lee, M. Taileb, A. Corella, S. Kilinc, J. Williams, M.L. Jokisch, R. Camarda, S. Balakrishnan, R. Shankar, A. Zhou, A.N. Chang, B. Chen, H.S. Rugo, S. Dumont, and A. Goga. 2020. MYC Dysregulates Mitosis, Revealing Cancer Vulnerabilities. *Cell reports*. 30:3368-3382.e3367.
- Sachs, N., J. de Ligt, O. Kopper, E. Gogola, G. Bounova, F. Weeber, A.V. Balgobind, K. Wind, A. Gracanin, H. Begthel, J. Korving, R. van Boxtel, A.A. Duarte, D. Lelieveld, A. van Hoeck, R.F. Ernst, F. Blokzijl, I.J. Nijman, M. Hoogstraat, M. van de Ven, D.A. Egan, V. Zinzalla, J. Moll, S.F. Boj, E.E. Voest, L. Wessels, P.J. van Diest, S. Rottenberg, R.G.J. Vries, E. Cuppen, and H. Clevers. 2018. A Living Biobank of Breast Cancer Organoids Captures Disease Heterogeneity. *Cell*. 172:373-386.e310.
- Smith, J.A., L. Wilson, O. Azarenko, X. Zhu, B.M. Lewis, B.A. Littlefield, and M.A. Jordan. 2010. Eribulin binds at microtubule ends to a single site on tubulin to suppress dynamic instability. *Biochemistry*. 49:1331-1337.
- Sousa, A., R. Reis, P. Sampaio, and C.E. Sunkel. 2007. The Drosophila CLASP homologue, Mast/Orbit regulates the dynamic behaviour of interphase microtubules by promoting the pause state. *Cell motility and the cytoskeleton*. 64:605-620.
- Su, S., G. Chhabra, C.K. Singh, M.A. Ndiaye, and N. Ahmad. 2022. PLK1 inhibition-based combination therapies for cancer management. *Translational oncology*. 16:101332.
- Thomas, G.E., J.S. Sreeja, K.K. Gireesh, H. Gupta, and T.K. Manna. 2015. +TIP EB1 downregulates paclitaxel-induced proliferation inhibition and apoptosis in breast cancer cells through inhibition of paclitaxel binding on microtubules. *Int J Oncol*. 46:133-146.
- Topham, C., A. Tighe, P. Ly, A. Bennett, O. Sloss, L. Nelson, R.A. Ridgway, D. Huels, S. Littler, C. Schandl, Y. Sun, B. Bechi, D.J. Procter, O.J. Sansom, D.W. Cleveland, and S.S. Taylor. 2015. MYC Is a Major Determinant of Mitotic Cell Fate. *Cancer Cell*. 28:129-140.
- Ueda, A., K. Oikawa, K. Fujita, A. Ishikawa, E. Sato, T. Ishikawa, M. Kuroda, and K. Kanekura. 2019. Therapeutic potential of PLK1 inhibition in triple-negative breast cancer. *Laboratory Investigation*. 99:1275-1286.
- van de Wetering, M., H.E. Francies, J.M. Francis, G. Bounova, F. Iorio, A. Pronk, W. van Houdt, J. van Gorp, A. Taylor-Weiner, L. Kester, A. McLaren-Douglas, J. Blokker, S. Jaksani, S. Bartfeld, R. Volckman, P. van Sluis, V.S. Li, S. Seepo, C. Sekhar Pedamallu, K. Cibulskis, S.L. Carter, A. McKenna, M.S. Lawrence, L. Lichtenstein, C. Stewart, J. Koster, R. Versteeg, A. van Oudenaarden, J. Saez-Rodriguez, R.G. Vries, G. Getz, L. Wessels, M.R. Stratton, U. McDermott, M. Meyerson, M.J. Garnett, and H. Clevers. 2015. Prospective derivation of a living organoid biobank of colorectal cancer patients. *Cell*. 161:933-945.
- Weaver, B.A. 2015. How Taxol/paclitaxel kills cancer cells. *Mol Biol Cell*. 25:2677-2681.
- Wissing, M.D., M.A. Carducci, H. Gelderblom, and P.J. van Diest. 2013. Tales of how great drugs were brought down by a flawed rationale--letter. *Clin Cancer Res*. 19:1303.

- Xie, S., A. Ogden, R. Aneja, and J. Zhou. 2015. Microtubule-Binding Proteins as Promising Biomarkers of Paclitaxel Sensitivity in Cancer Chemotherapy. *Medicinal research reviews*.
- Yang, G., A. Matov, and G. Danuser. 2005. Reliable tracking of large scale dense antiparallel particle motion for fluorescence live cell imaging. *In Proc. IEEE Computer Vision and Pattern Recognition*, San Diego. 138-146.
- Ye, A.A., and T.J. Maresca. 2013. Cell division: kinetochores SKAdaddle. *Current biology : CB*. 23:R122-124.
- Zasadil, L.M., K.A. Andersen, D. Yeum, G.B. Rocque, L.G. Wilke, A.J. Tevaarwerk, R.T. Raines, M.E. Burkard, and B.A. Weaver. 2014. Cytotoxicity of paclitaxel in breast cancer is due to chromosome missegregation on multipolar spindles. *Sci Transl Med*. 6:229ra243.
- Zhang, R., G.M. Alushin, A. Brown, and E. Nogales. 2015. Mechanistic Origin of Microtubule Dynamic Instability and Its Modulation by EB Proteins. *Cell*. 162:849-859.